


Article

Elaboration of a Multi-Objective Optimization Method for High-Speed Train Floors Using Composite Sandwich Structures

Mortda Mohammed Sahib ^{1,2} and György Kovács ^{1,*} ¹ Faculty of Mechanical Engineering and Informatics, University of Miskolc, 3515 Miskolc, Hungary; mortda.inst@stu.edu.iq² Basrah Technical Institute, Southern Technical University, Basrah 610016, Iraq

* Correspondence: gyorgy.kovacs@uni-miskolc.hu

Abstract: The transportation industry needs lightweight structures to meet economic and environmental demands. Composite sandwich structures offer high stiffness and low mass, making them ideal for weight reduction in high-speed trains. The objective of this research is to develop a method of weight and cost optimization for floors of high-speed trains. The studied sandwich floor structure consists of Fiber Metal Laminates (FML) face sheets and a honeycomb core. Different variations of FMLs were investigated to define the optimal sandwich structure for minimum weight and cost. The Neighborhood Cultivation Genetic Algorithm (NCGA) was used to search the design space, and the Finite Element Method (FEM) was used to construct the optimal design of the train car floor panel. The FEM and optimization results had a maximum difference about 11%. The study concluded that using face sheets made entirely of Fiber-Reinforced Plastic (FRP) or Fiber Metal Laminates (FMLs) resulted in significant weight savings of approximately 62% and 32%, respectively, compared to a sandwich structure made entirely of aluminum, but a lighter structure was associated with higher cost. The main contribution of this study is the elaboration of a multi-objective optimization method that utilizes a wide range of constituent materials and structural components in order to construct weight- and cost-optimized sandwich structures.

Keywords: sandwich structure; fiber metal laminates; optimization; NCGA algorithm; train floor



Citation: Sahib, M.M.; Kovács, G. Elaboration of a Multi-Objective Optimization Method for High-Speed Train Floors Using Composite Sandwich Structures. *Appl. Sci.* **2023**, *13*, 3876. <https://doi.org/10.3390/app13063876>

Academic Editor: Camelia Cerbu

Received: 1 March 2023

Revised: 14 March 2023

Accepted: 16 March 2023

Published: 18 March 2023



Copyright: © 2023 by the authors. Licensee MDPI, Basel, Switzerland. This article is an open access article distributed under the terms and conditions of the Creative Commons Attribution (CC BY) license (<https://creativecommons.org/licenses/by/4.0/>).

1. Introduction

Weight reduction of rail vehicles has gained considerable importance with the development of rail transportation [1,2]. In order to meet the basic requirements of rail vehicles while reducing their weight, producing innovative panel structures has gained considerable importance [3,4].

In recent years, sandwich structures have played a significant role in innovative practical applications due to their low density and high structural performance. Research on the optimization of these sandwich structures for various industrial applications is receiving increasing attention [5,6]. A sandwich composite structure (Figure 1) consists of two thin, highly rigid face sheets that are separated by a lightweight core. The core material usually has low mechanical properties, but its greater thickness results in high structural stiffness and strength [7–9].

A review of the literature has shown that research on sandwich structures has been approached from different perspectives. Sayyad and Ghugal studied the bending, buckling, and free vibration of sandwich structures using different analytical models [10]. Liu et al. studied the crash behavior of sandwich structures consisting of aluminum honeycomb cores filled with expanded polypropylene foam (EPP) under both in-plane and out-of-plane compressive loads [11]. Kwon et al. investigated the optimization of the interface between the epoxy foam core and the Carbon Fiber-Reinforced Plastic (CFRP) face sheets in a sandwich structure to improve the compressive and impact properties of the final

sandwich structure [12]. In another study, Mohammed et al. achieved the optimization of the bottom panel of a heavy truck, which focused on a composite sandwich structure under distributed out-of-plane loads. Their results showed that replacing the face sheet of the sandwich structure with CFRP material resulted in a significant weight reduction [13]. Seyyedrahmani et al. proposed a framework for the optimization of laminated sandwich panels by addressing a multi-objective optimization problem considering cost, dynamic behavior, and carrying load. The authors presented Pareto-optimal solutions and identified the design points that provide the best trade-off [14].

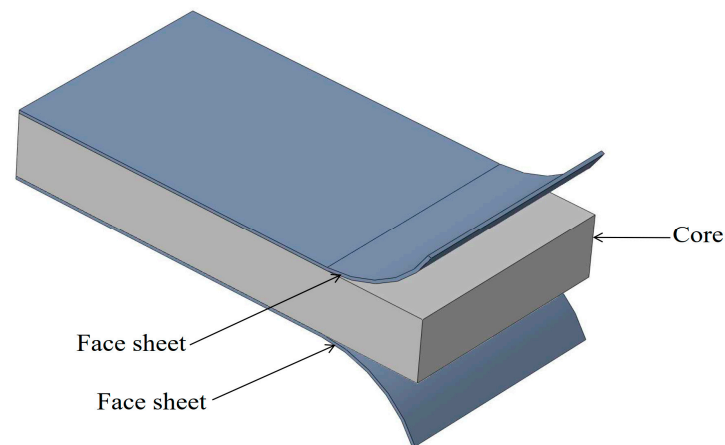


Figure 1. Components of the sandwich panel.

In the railway field, many investigations have been carried out from different points of view. Manalo and Aravinthan performed shear and bending tests on composite sandwich structures for rail sleeper applications. They concluded that the composite sandwich structures could potentially replace conventional railway sleepers [15]. In another study, Cho et al. investigated the weight optimization of a car body for a transit train based on material selection and size optimization procedures for the components of the car body, such as the roof, side walls, and subframe. The study found that the use of sandwich structures resulted in a significant weight reduction of up to 29% [16]. Zinno et al. proposed a multiscale design approach for sandwich composite structures on rail vehicle roofs. Experimental, theoretical, and numerical analyses were used to optimize the structural design in terms of cost efficiency [17].

In another study, Heller et al. used Glass Fiber-Reinforced Plastic (GFRP) sandwich composites to fabricate railcar ceiling panels and walls and demonstrated an overall weight reduction of 20% compared to conventional stainless steel ceiling panels and sidewalls [18]. Yao et al. developed a lightweight construction approach to improve the sound insulation of floating floors in rail vehicles. The authors optimized several variables, reduced the mass by 15.2%, and significantly increased the sound insulation [19]. Wennberg and Stichel proposed a multifunctional optimization for the body of high-speed trains. They achieved a weight reduction of up to 17% by using composite sandwiches, while also meeting the thermal, fire protection, and acoustic requirements [20].

Mozafari et al. investigated the effects of using foam-filled sandwich panels on the energy absorption and impact resistance of rail vehicles. The results showed that polyurethane foam filling can significantly increase crushing strength and energy absorption capacity. However, the weight of the car body increased by only 2% [21].

Reducing the cost of composites while improving their properties remains an attractive motivation in the field of composite development [22]. Fiber Metal Laminates (FMLs) have shown significant potential for optimizing structures by combining metal sheets and Fiber-Reinforced Plastic (FRP) composite laminates to provide a range of benefits from each material group. Thus, FMLs offer an excellent opportunity for creating lightweight structures [23]. The properties and failure modes of FMLs were studied by Gao et al.

They performed three-point bending tests to analyze the bending behavior of CARbon fiber-Reinforced composites/Aluminum Laminates (CAR-ALLs) with different composite/metal layer configurations [24]. Vieira et al. investigated the impact behavior of SiRALs (aluminum laminates reinforced with sisal fibers) and evaluated the influence of fiber orientation on performance [25].

Numerous studies have investigated the use of sandwich composite structures in railway [15–21]. However, in terms of weight and cost optimization of the train floor, few have attempted to provide an accurate analytical model that can offer the optimal configuration of honeycomb cores and face sheets from a variety of possible combinations to achieve the best trade-off between weight reduction and cost efficiency.

In this study, we elaborate an integrated approach to make new contributions, as described below:

1. **Material selection:** In this study, different types of aluminum (Al) honeycomb cores are used in combination with different combinations of Fiber Metal Laminates (FMLs) as face sheets. This particular combination of materials and structural components had not been investigated in the literature before.
2. **Cost and weight optimization:** The elaborated optimization procedure in this study focuses on weight and cost, since only a limited number of previous studies have investigated the relationship between weight and cost reduction simultaneously.
3. **Flexible design:** A wide range of design variables is used in our study to investigate a larger number of feasible designs and determine the optimal sandwich construction.
4. **Structural integrity:** The optimization method used in this study effectively satisfies the specified constraints on the strength of the sandwich structure and the behavior of the final sandwich structure.
5. **New optimization algorithm:** The application of the NCGA algorithm for the structural optimization of floors for high-speed trains represents a new contribution that is not represented in the literature. This highlights the ability of the NCGA algorithm to achieve optimal designs that balance weight reduction and cost efficiency.

The paper is organized as follows: Section 2 provides a basic description of the investigated train floor, while Section 3 explains the materials used in the examined sandwich structures and their mechanical properties. The optimization problem and the mathematical models for objective functions, design constraints, and design variables are discussed in Section 4. Section 5 describes the creation of a finite element model for the optimal designs. The structural optimization results are presented in Section 6. Finally, Section 7 highlights the main conclusions of this study.

2. Description of the Investigated Train Floor

Figure 2 illustrates the floor structure of a high-speed train, which consists of an aluminum structure as part of the main vehicle structure on the exterior, and a series of sub-panels supported by seats with hard rubber to reduce vibrations on the interior. The subpanel model can be considered as a unit of the floor. This study focuses on the subpanel, which is considered as a sandwich structure (inner floor) with a lightweight honeycomb core and two face sheets, as shown in Figures 2 and 3.

In this study, the investigated sandwich of internal floor subpanel has a longitude length (l) of 960 mm and a transverse length (b) of 582 mm. Each subpanel is installed on four supporting seats. Without considering fatigue effects of the floor, it can be assumed that the loads are evenly distributed. The value of the load (p) acting on the floor is estimated to be 4.142 kPa [26]. The subpanel was selected as a representative structure to study the loading conditions of the sandwich structure. By analyzing the behavior of the subpanel, the study aims to gain insights into the performance of the overall sandwich structure. The loading condition of the floor subpanel implies that the sandwich structure is simply supported by support seats and subjected to a distribution load in the out-of-plane direction, as shown in Figure 3.

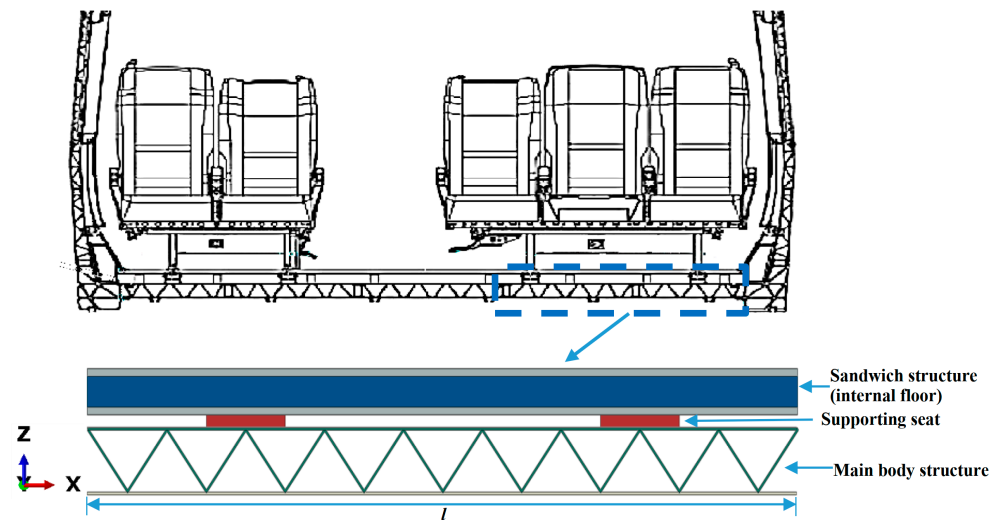


Figure 2. Structure of the high-speed train floor and the investigated subpanel.

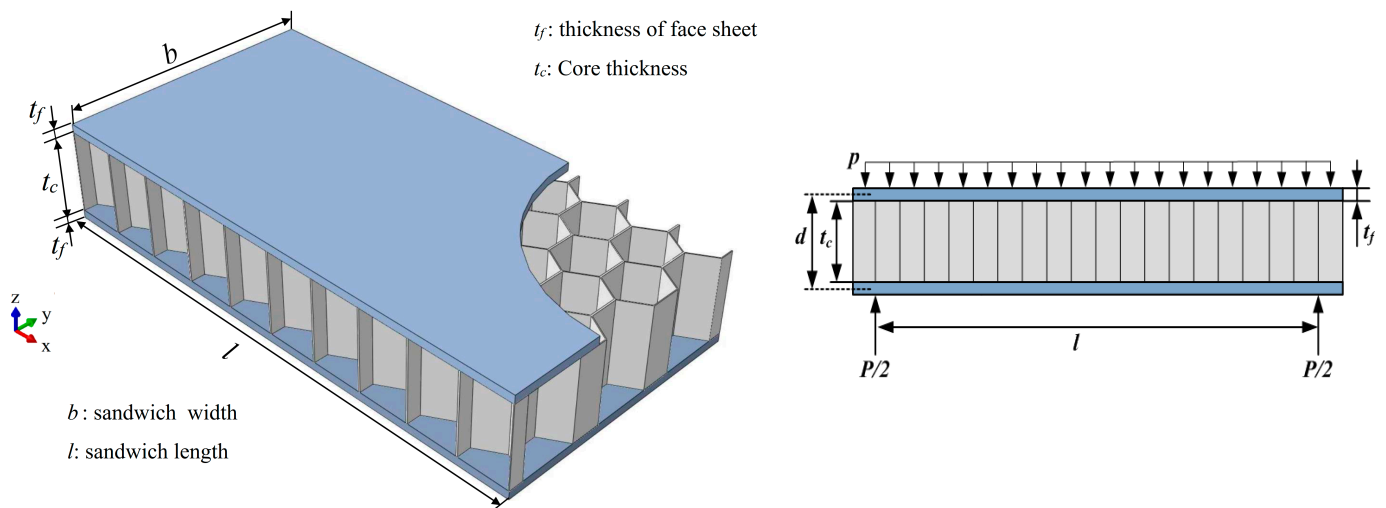


Figure 3. Loading and boundary condition of the investigated sandwich structure.

3. Materials of the Sandwich Structure's Components

3.1. Materials of the Face Sheets

In this study, the subpanel of the train floor was analyzed as a sandwich structure consisting of hybrid composite face sheets made of Fiber Metal Laminates (FML) and an Aluminum (Al) honeycomb core. In recent years, Fiber Metal Laminates have gained considerable attention among the families of Fiber-Reinforced Plastic (FRP) composites. FMLs are composites composed of alternating layers of metal sheets or foils and Fiber-Reinforced Plastic layers bonded together by thermal pressing technique [27]. Figure 4 shows the alternating structure of an FML. Classical Lamination Theory (CLT) has been proposed model to calculate the final mechanical properties of FMLs [28]. This approach offers the possibility of adjusting the properties of the laminated face sheets by changing the number of face sheet layers and also the orientation of FRP layers, as will be explained in the following section.

When using FMLs, it is important to consider that the hybridization of composite face sheets with FML laminates is a powerful technique for developing composite structures that provide the desired cost and/or weight reduction while effectively improving the stiffness properties. In our study, FMLs were composed of (1) Carbon Fiber-Reinforced Plastic (CFRP), (2) Glass Fiber-Reinforced Plastic (GFRP), and (3) Aluminum (Al). These face sheets consist of layers of unidirectional CFRP, GFRP, and AL, which are arranged

in different orders. As depicted in the right side of Figure 4, the possible orientations of the FRP layers can be 0° , $\pm 45^\circ$, and 90° in the laminated face sheet. The final mechanical properties of the laminated face sheets were calculated using Classical Lamination Theory. Table 1 shows the possible constituent materials properties of the Fiber Metal Laminates that were considered in the optimization [29].

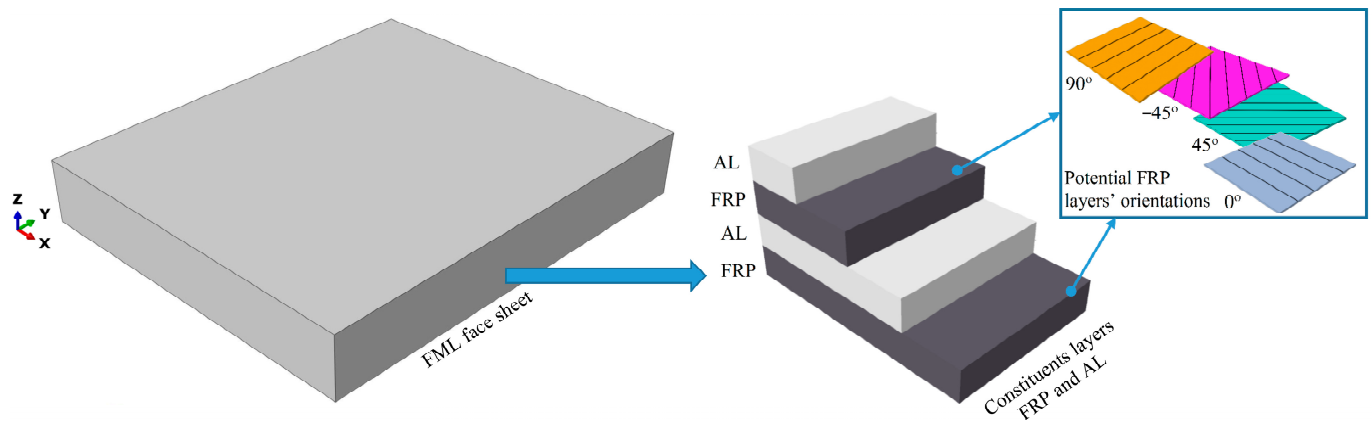


Figure 4. Face sheet layup with FML material.

Table 1. Material properties of the possible constituents of the FML face sheets.

Material Properties	CFRP	GFRP	AL
Longitudinal modulus: E_x [MPa]	130,000	43,000	70,000
Transverse modulus: E_y [MPa]	10,000	8000	70,000
In-plane shear modulus: G_{xy} [MPa]	5000	4300	26,000
Major Poisson's ratio: ν_{xy} [-]	0.28	0.25	0.33
Density: ρ_f [kg/m ³]	1600	1800	2780
Lamina thickness: t_l [mm]	0.125	0.125	0.2
Longitudinal tensile strength: σ_{xt} [MPa]	2000	1140	186
Longitudinal compressive strength: σ_{xc} [MPa]	1300	620	186
Transverse tensile strength: σ_{yt} [MPa]	78	39	186
Transverse compressive strength: σ_{yc} [MPa]	246	128	186
In-plane shear strength: σ_{xy} [MPa]	68	60	110

3.2. Material of the Honeycomb Core

The honeycomb core is also a critical component during the optimization of the sandwich structure because its mechanical properties are proportional to its density. Therefore, commercially available core densities were utilized in the analysis. Table 2 presents the mechanical properties of the aluminum hexagonal honeycomb core [29].

Table 2. Mechanical properties of aluminum hexagonal core.

Density	Properties in x Direction		Properties in y Direction		Properties in z Direction	
ρ_c [kg/m ³]	Strength: σ_{xx} [MPa]	Modulus: G_{xx} [MPa]	Strength: σ_{yy} [MPa]	Modulus: G_{yy} [MPa]	Strength: σ_{zz} [MPa]	Modulus: E_{zz} [MPa]
29	0.4	55	0.65	110	0.9	165
37	0.45	90	0.8	190	1.4	240
42	0.5	100	0.9	220	1.5	275
54	0.85	130	1.4	260	2.5	540
59	0.9	140	1.45	280	2.6	630
83	1.5	220	2.4	440	4.6	1000
29	0.4	55	0.65	110	0.9	165
37	0.45	90	0.8	190	1.4	240
42	0.5	100	0.9	220	1.5	275
54	0.85	130	1.4	260	2.5	540

4. Elaboration of the Optimization Method

The main aim of composite sandwich structure optimization is to minimize the structural weight and cost while achieving the structural integrity of the optimized structure. This paper considers weight and cost objective functions to optimize a high-speed train's floor by using a lightweight composite sandwich structure. It is worth mentioning that the investigated objective functions are in conflict with each other, so the multi-objective optimization problem is formulated with the associated design variables and design constraints. It is essential that the components of the sandwich structure have sufficient strength to withstand the applied loads; therefore, strength has been defined as one of the design constraints. The investigated sandwich structure consisted of hybrid laminates (FML) for the face sheets and an aluminum honeycomb core.

The objective functions applied in this paper involve the minimization of both the weight and cost of the composite sandwich structure. In the context of the floor structure under consideration, the aim was to identify the Pareto solution of sandwich constructions that are optimal for achieving low weight and low cost simultaneously.

During the optimization, the optimal material constituents and geometrical parameters of the components (face sheets and core) were sought for a given practical application in case of the given loading conditions.

The optimization procedure was managed using the Neighborhood Cultivation Genetic Algorithm (NCGA) optimization algorithm, which was implemented through the I-sight software environment integrated with Excel software. The main steps of the optimization and FEM validation processes are illustrated in the flowchart shown in Figure 5.

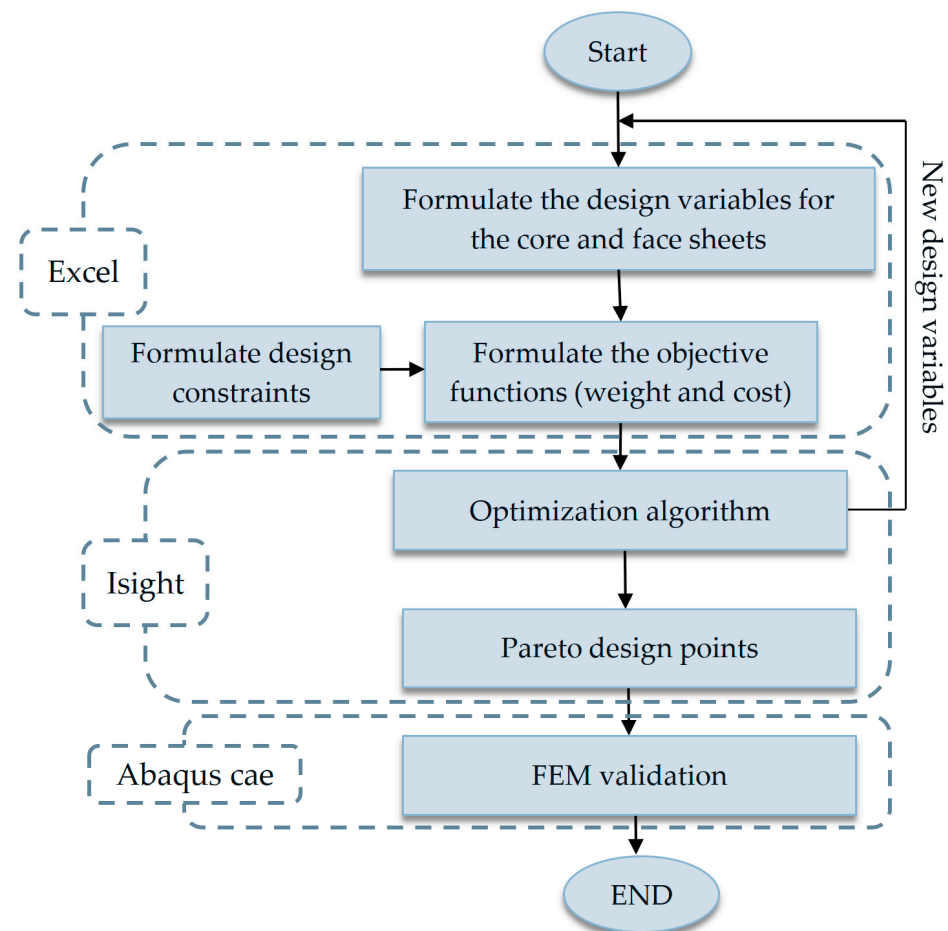


Figure 5. Flowchart of the elaborated multi-objective optimization method for the investigated composite sandwich structure.

During the optimization, the Neighborhood Cultivation Genetic Algorithm (NCGA) was applied to obtain an optimal sandwich construction. In this technique, each objective function is treated separately and a Pareto front is constructed by selecting feasible non-dominated designs. NCGA is particularly suitable for discrete multi-objective problems and has been shown to provide a robust solution. The computational process of NCGA consists of several steps as it illustrated in Table 3 [30]:

Table 3. NCGA flow steps and descriptions.

Steps	Process Description
Step 1.	Initialization —In this step, an initial population P_0 of size N is established, and the generation is set to an initial value of $g = 0$. The fitness values associated with individuals in P_0 are calculated, and P_0 is copied into an archive A_0 of size N .
Step 2.	Generation —A new generation is created by incrementing the generation counter ($g = g + 1$) and selecting the parent population (P_g) from the previous archive (A_{g-1}).
Step 3.	Sorting —The population is sorted based on the specified objectives for the current generation. If optimizing for two objective functions, the first objective is chosen in the first generation, the second objective in the second generation, and so on.
Step 4.	Grouping — P_g is split into two groups consisting of stored individuals.
Step 5.	Crossover and Mutation —Crossover and mutation operations are performed on each group, producing two child individuals from two parent groups and then eliminating the parent groups.
Step 6.	Assembly —The child groups generated in Step 5 are assembled to produce a new population (P_g).
Step 7.	Archive Renewal — P_g and A_{g-1} are combined to generate $2N$ individuals. Environment selection is then conducted to reduce the number of individuals to N , and a new archive (A_g) is generated.
Step 8.	Termination —The terminal criterion is verified. If the criterion has been met, the process can be stopped. If not, the algorithm returns to Step 2.

It is common for multi-objective optimizations not to find a single optimal solution, but to have multiple solutions, each containing an element of optimality, which is referred to as Pareto-optimal solutions [31]. The Pareto solution refers to a set of optimal solutions that fulfill the specified objectives. However, further selection is required to determine the best solution [32]. Therefore, in this study, the Improved Minimum Distance Selection Method (IMDSM) [33] was used to determine the most satisfactory point, referred to as the knee point. The knee point can be expressed as follows:

$$D_{min} = \sqrt{\left(\frac{f_{W_t}(x)}{\min(f_{W_t}(x))} - 1\right)^2 + \left(\frac{f_{C_t}(x)}{\min(f_{C_t}(x))} - 1\right)^2}, \quad (1)$$

where D_{min} represents the minimum distance from the ideal point (minimum weight, minimum cost) to any point on the Pareto line, $f_{W_t}(x)$ refers to the value of the weight objective function on the Pareto line, and $f_{C_t}(x)$ represents the value of the cost objective function on the Pareto line. D_{min} was calculated for 13 values, which corresponds to the number of Pareto points. However, the minimum distance value was identified to be the optimal solution.

4.1. Weight and Cost Objective Functions

During the structural optimization, the weight and the cost objective functions were taken into consideration.

4.1.1. Weight Objective Function

The total weight of the structure is composed of the weight of the two face sheets and the weight of the core. The total weight of the structure is given by:

$$W_t = W_c + W_f = \left(\rho_c t_c + 2 \left(\rho_{f1} N_{l1} t_{l1} + \rho_{f2} N_{l2} t_{l2} + \rho_{f3} N_{l3} t_{l3} \right) \right) lb \quad (2)$$

where W_t is the total weight of the sandwich structure, W_c is the weight of the honeycomb core, and ρ_c and t_c are the density and thickness of the aluminum honeycomb core, respectively. W_f is the weight of the face sheet; indices 1, 2, and 3 refer to CFRP, GFRP, and AL respectively, while ρ_f , N_l , and t_l are the density, number of layers, and thicknesses of each of the constituent materials.

The total thickness of the face sheet (t_f), which is composed of the stacked layers of individual constituent materials, can be calculated by:

$$t_f = N_{l1} t_{l1} + N_{l2} t_{l2} + N_{l3} t_{l3}. \quad (3)$$

4.1.2. Cost Objective Function

The total cost of the structure is the sum of the cost of the two face sheets and the cost of the core:

$$C_t = C_f + C_c, \quad (4)$$

where C_t is the total cost of the sandwich structure, and C_f and C_c are the costs of the face sheet's layers and cost of the core. In order to estimate the costs of the constituent materials in a sandwich structure, a deep survey was conducted as part of this study. In the interest of generalization, the unit price of each material was normalized to the price of GFRP. The cost of CFRP, the core, and aluminum were reported as 1.5, 0.5, and 0.31 times the cost of GFRP, respectively.

4.2. Design Variables

The design variables are the main characteristics of the sandwich structure. These design variables include face sheets composed of different FRP composite materials such as CFRP and GFRP, as well as aluminum layers. The face sheets are characterized as FLM laminates and their final properties are determined by the orientation of the fibers associated with FRP composite laminates, the number of layers, and the final face sheet thickness. Furthermore, the selection of the honeycomb core density varied within a wide range. The aforementioned design variables are summarized in Table 4.

Table 4. Design variables of the optimization.

Design Variables	Value	Remark
Number of face sheet layers	$1 \leq N_l \leq 15$	Discrete variable, Integer values
Face sheet materials	CFRP layer: identified by No. 1 GFRP layer: identified by No. 2 Aluminum layer: identified by No. 3	Discrete variable, Integer values
possible FRP composite layup orientation	$\theta_{FRP} = 0^\circ, 90^\circ, +45^\circ, -45^\circ$	Discrete variable
Core density	ρ_c [kg/m ³]	Discrete as specified in the Table 2
Core thickness	$5 \leq t_c \leq 20$ [mm]	Continuous value

4.3. Design Constraints

In order to perform effective optimization, it is necessary to distinguish between sandwich constructions that are aligned with a specific purpose and those that are not. In other words, design constraints are the limitations that any proposed design must comply with.

In this study, design constraints such as maximal deflection of the structure, strength limitations, and failure criteria for the sandwich structure were used to establish the necessary limits that any proposed design must satisfy.

4.3.1. Constraint for Core Shear

The honeycomb core is subjected to shear stress in the considered loading condition. Therefore, a shear constraint can be formulated as follows:

$$\frac{\tau_{cs}}{\tau_c} \geq 1.0, \quad (5)$$

where τ_{cs} is the typical shear strength of the core as listed in Table 2. the inferred shear stress in the core (τ_c) can be formulated by [34,35]:

$$\tau_c = \frac{F}{db}, \quad (6)$$

where F and b are the shear force and sandwich structure's width, respectively, whereas d is the distance between the upper and lower face sheets' centers. d can be calculated as below [34,35]:

$$d = t_f + t_c. \quad (7)$$

4.3.2. Constraint for Yield Stress in the Face Sheet

The mathematical formulation of the constraint for the yielding of the face sheet is expressed as [34,35]:

$$\frac{\sigma_x}{\sigma_f} \geq 1.0. \quad (8)$$

The yield strength of the laminated face sheet (σ_x) was calculated by applying the Tsai–Wu failure criterion and the Classical Lamination Theory (CLT), as described in [36]. The stress in the face sheet (σ_f) and the maximum bending moment can be determined using the below equations [34,35]:

$$\sigma_f = \frac{M_{max}}{bdt_f}, \quad (9)$$

where the maximum moment (M_{max}) can be calculated using the following formula:

$$M_{max} = P \frac{l}{8}, \quad (10)$$

where l is the length of sandwich structure; the effective vertical force (P) is calculated by [34,35]:

$$P = plb, \quad (11)$$

where p refers to the distribution load in the upper face sheet.

4.3.3. Constraint for Face Wrinkling

Under in-plane shear or compression loading conditions, the sandwich structure may experience local buckling waves, resulting in a phenomenon known as face wrinkling. The criterion for in-plane wrinkling in two directions can be expressed as follows, according to [35]:

$$\frac{\sigma_{wr,x}}{\sigma_x} \geq 1.0 \quad (12)$$

$$\sigma_{wr,x} = 0.5 \sqrt[3]{E_x E_{zz} G_{xz}} \quad (13)$$

$$\frac{\sigma_{wr,y}}{\sigma_y} \geq 1.0 \quad (14)$$

$$\sigma_{wr,y} = 0.5 \sqrt[3]{E_y E_{zz} G_{yz}}, \quad (15)$$

where $\sigma_{wr,x}$ and $\sigma_{wr,y}$ are the wrinkling stress in the x and y directions, and the other parameters are defined in Tables 1 and 2.

4.3.4. Constraint for Total Thickness of the Sandwich Structure

A constraint for the total thickness of the sandwich structure, which should not exceed 20 mm, can be mathematically expressed as follows [26]:

$$H = 2t_f + t_c \leq 20, \quad (16)$$

where H is the sum of the core thickness and the face sheets' thickness.

4.3.5. Constraint for Total Deflection of the Sandwich Structure

The total deflection is contributed by both bending deflection and shear deflection, as indicated in [34,35,37]:

$$\delta = \frac{5 Pl^3}{384 D} + \frac{Pl}{8S} \leq 1. \quad (17)$$

The bending (D) and shear stiffness (S) can be determined using the following formulas:

$$D = \frac{E_f t_f b d^2}{2} \quad (18)$$

$$S = dbG_{xz}. \quad (19)$$

5. Numerical Modelling of the Investigated Structure

The aim of the numerical modeling was to confirm the accuracy of the developed optimization method. A commercial Finite Element package, ABAQUS/CAE, was used for the numerical modeling of the sandwich structure. Despite its higher computational cost, we believe that using ABAQUS/CAE provides greater flexibility in terms of geometry and load cases, particularly when dealing with composite sandwich structures.

The honeycomb core material properties were defined in the "Material Properties" module and then assigned using the "Assign Section" module. The mechanical properties of the FML materials were defined for each individual constituent using the main engineering constants listed in Table 1. The FML composite was simulated using the "composite layup" function in ABAQUS, which allows for the definition of the layers' sequences of the FML laminate and the fiber orientations in each FRP layer. To reduce the computational cost of the sandwich structure, the honeycomb core was simulated as a solid layer with homogeneous mechanical properties of the detailed honeycomb core [38,39]. Therefore, the three-dimensional stress element C3D8R was used to simulate the aluminum honeycombs.

The common shell element S4R was used to simulate the laminated composite face sheets. A general contact with a tangential friction property and a normal "hard" contact was specified. The honeycomb core was meshed with 2925 solid elements, while 4557 shell elements were created to mesh the face sheets. The distribution load defined in Section 2 was applied to the upper face. The geometric model of the support seats was also modeled and defined as a rigid body. A coupling constraint between the support seats and the reference points (RP) was used, and then a fully fixed constraint was applied to RP, which follows the fixation nature of the subpanel. As highlighted in Section 4, the failure criterion of the face sheets was considered a crucial optimization constraint. Therefore, non-feasible designs that did not meet the failure criterion were excluded from further analysis. Conversely, all feasible designs that fulfilled the failure constraints can be adopted under elastic load conditions that are significantly lower than the failure load. Based on these considerations, the current FEM model was created to validate the optimization results without considering the failure of the FML face sheet. This fact is evident in the results section, as the stresses of the face sheet layers are significantly lower than the failure strength of each constituent. The main parameters for optimal design points used in FEM modeling are elaborated in

Section 6, while the general FEM model of the composite sandwich structure is shown in Figure 6.

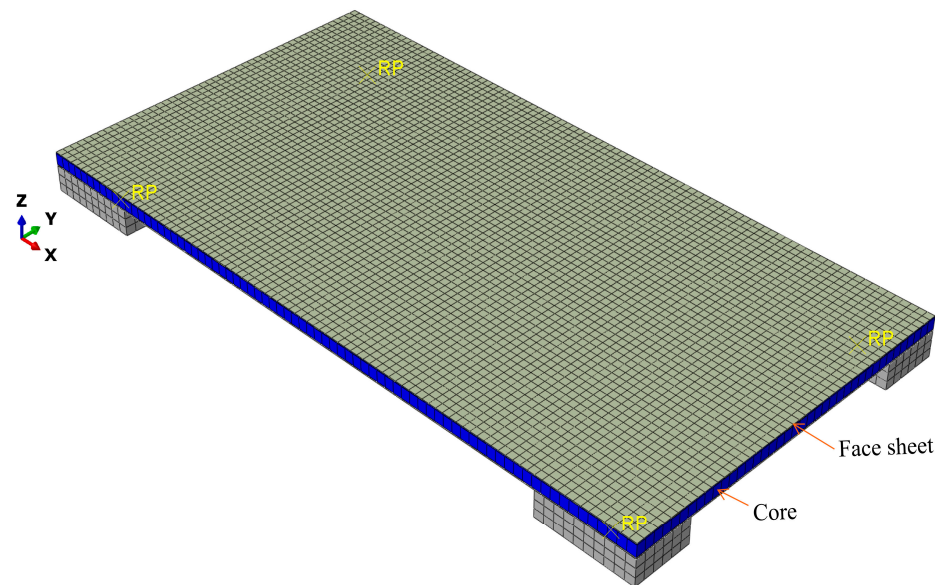


Figure 6. Finite Element Model of the investigated train floor.

6. Results of the Optimization and the Finite Element Modeling

6.1. Results of the Elaborated Optimization Method

In contrast to single-objective optimization problems, the solution of a multi-objective optimization problem is not unique. Instead, a range of optimal solutions can be considered. In multi-objective optimization, the improvement of one objective may lead to the deterioration of the performance of the other objectives. Therefore, it is difficult to achieve multiple optimal values simultaneously, and the only way to do that is to make each objective as optimal as possible.

Consistent with the formulation of the multi-objective optimization problem in Equations (2) and (4), the objectives of sandwich structure optimization were defined as reducing the overall weight (W_t) and cost (C_t) while ensuring the durability of the structure. In this study, different densities of honeycomb cores and hybridized face sheets (FML) with their associated parameters were used as design variables to achieve the final objectives. Since the contradiction between the total weight of the sandwich structure and the cost was obvious, we chose the Neighborhood Cultivation Genetic Algorithm to investigate the optimal solution using I sight software in conjunction with Excel software.

The total number of feasible solutions for this study was approximately 16,600 design points. The changes in weight and cost in the optimized design are shown in Figure 7. The blue hollow circles represent the feasible solutions of the optimization problem, which satisfy all the constraints of the problem while achieving a certain level of performance with respect to multiple competing objectives. The green solid circles represent the set of non-dominated solutions, which achieve the best trade-off between multiple competing objectives, also known as the Pareto set, and represent the best solutions of the optimization problem. The NCGA algorithm acquired 13 data points, which were extracted in Figure 8 and represent the Pareto set.

Pareto points tend to be convexly distributed due to the opposing objectives' behavior. Whenever the weight decreases, the cost of the sandwich structure increases and vice versa. Therefore, the knee point was considered the most satisfactory solution. The calculations showed that the knee point with $W_t = 5.25$ kg and $C_t = 2.37$ unit price should be appointed as the optimal solution, representing an ideal compromise between the opposite objectives. The corresponding Pareto data are shown in Table 5.

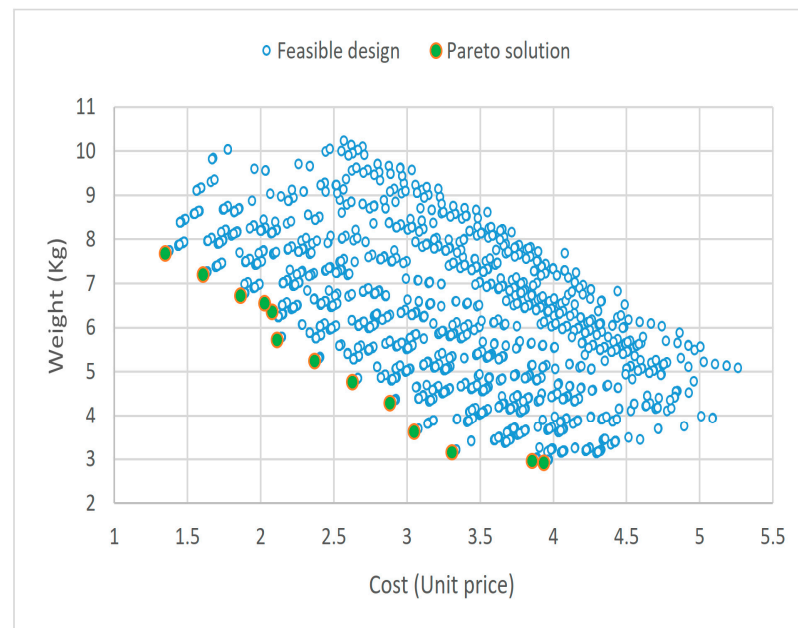


Figure 7. Feasible design points.

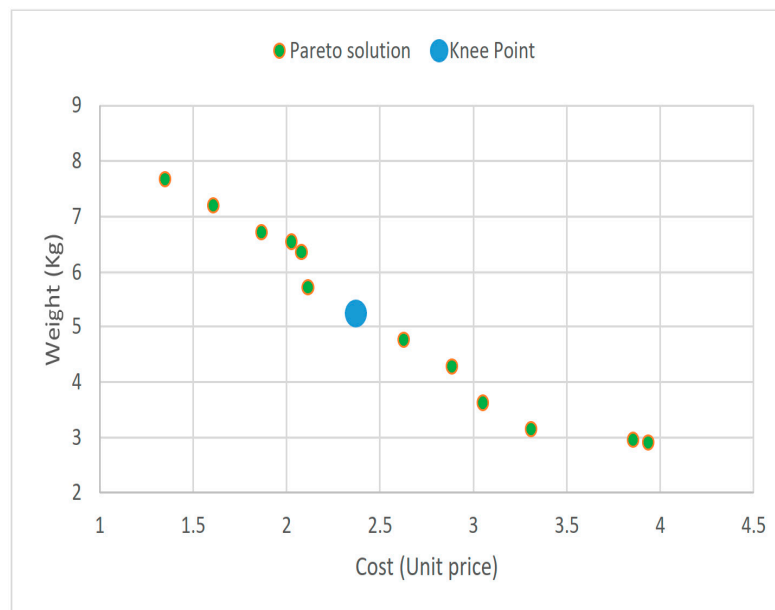


Figure 8. Pareto optimal points.

The minimum weight, minimum cost, and knee design points are the most significant design points on the Pareto line. Therefore, the related data have been extracted in Table 6 for further consideration. The data include the main parameters related to the geometrical characteristics of sandwich structure components and configurations, and have been adopted in the FEM modeling.

The optimization of weight and cost of sandwich structures is crucial, and the hybridization of face sheet materials has been shown to have a significant impact on achieving these objectives. One approach to achieving this is to create a hybrid structure that combines the strengths of various materials while complementing their weaknesses.

The cost and weight of a hybrid composite sandwich structure is determined by the sum of the cost and weight of its constituents. Therefore, the final composite face sheet is a function of the composite ratio of each material. In this study, the percentage of the FRP materials in terms of weight and cost was considered, as depicted in Figure 9. The

figure shows that a higher percentage of FRP results in a lighter and more expensive sandwich structure, whereas reducing the FRP materials tends to result in a heavier and less expensive structure.

Table 5. Results of the Pareto optimal design.

Face Sheet Materials and Fiber Orientations	No. of Layers	Core Thickness t_c	Face Sheet Thickness t_f	Core Density ρ_c	Cost C_t	Weight W_t
CFRP layer: identified by No. 1 GFRP layer: identified by No. 2 Aluminum layer: identified by No. 3		(mm)	(mm)	(kg/m ³)	(unit price)	(kg)
1(0°), 1(0°), 1(0°), 1(0°), 1(0°), 1(0°), 1(0°), 1(0°)	10	18.2	1.25	37	3.93	2.92
1(0°), 2(0°), 1(0°), 1(0°), 1(0°), 1(0°), 1(0°), 1(0°)	10	18.02	1.25	37	3.85	2.96
1(0°), 3, 1(0°), 1(0°), 1(0°), 1(0°), 1(0°), 1(0°)	9	18.47	1.2	37	3.31	3.15
1(0°), 3, 1(0°), 1(0°), 1(0°), 1(0°), 1(0°), 1(0°)	9	18.47	1.275	37	3.05	3.63
1(0°), 3, 1(0°), 1(0°), 1(0°), 3, 3, 1(0°), 1(0°)	9	17.88	1.35	54	2.88	4.29
3, 3, 1(0°), 1(0°), 1(0°), 1(0°), 3, 1(0°), 3	9	17.97	1.425	54	2.63	4.77
3, 3, 1(0°), 1(0°), 1(0°), 3, 3, 1(0°), 3	9	18.04	1.5	54	2.37	5.25
3, 3, 1(0°), 3, 1(0°), 3, 3, 1(0°), 3	9	18.13	1.575	54	2.11	5.73
3, 3, 3, 1(0°), 3, 3, 3, 1(0°), 3, 2(0°)	10	18.2	1.775	42	2.08	6.36
3, 3, 3, 3, 1(0°), 3, 3, 1(0°), 3	9	18.13	1.65	83	2.03	6.55
3, 3, 3, 1(0°), 3, 3, 3, 1(0°), 3, 3	10	17.8	1.85	37	1.86	6.72
3, 3, 3, 3, 3, 3, 3, 3, 3, 1(0°)	10	17.93	1.925	37	1.61	7.2
3, 3, 3, 3, 3, 3, 3, 3, 3, 3	10	17.94	2	37	1.35	7.68

Table 6. The design parameters for FEM simulation.

Face Sheet Layup	Face Sheet Materials and Fiber Orientations	No. of Layers	Core Thickness t_c	Face Sheet Thickness t_f	Core Density ρ_c	Values of the Objectives
	CFRP layer: No. 1 GFRP layer: No. 2 Aluminum layer: No. 3		(mm)	(mm)	(kg/m ³)	
Totally FRP	1(0°), 1(0°), 1(0°), 1(0°), 1(0°), 1(0°), 1(0°), 1(0°)	10	18.2	1.25	37	Minimal weight $W_t = 2.92$ kg $C_t = 3.93$ unit price
Totally Al	3, 3, 3, 3, 3, 3, 3, 3, 3, 3	10	17.94	2	37	Minimal cost $W_t = 7.68$ kg $C_t = 1.35$ unit price
FML	3, 3, 1(0°), 1(0°), 1(0°), 3, 3, 1(0°), 3	9	18.04	1.5	54	Knee point $W_t = 5.25$ kg $C_t = 2.37$ unit price

Furthermore, a comparison was conducted between a train floor made of a totally Al structure, a totally FRP structure, and a FML structure in terms of weight and cost. The optimal material selection (Table 6) showed that the maximum weight reduction among the considered designs was about 62%, while the associated cost increased by about 190% with the use of Carbon Fiber-Reinforced Plastic (CFRP) as the face sheet material. The knee point was reached at a weight reduction of 32% and a cost increase of 75% compared to an all-Al structure.

It is important to note that, although the weight reduction was achieved at the expense of cost, the benefits of reduced weight include lower energy consumption and lower maintenance costs in the long run, resulting in a significant cost savings over time.

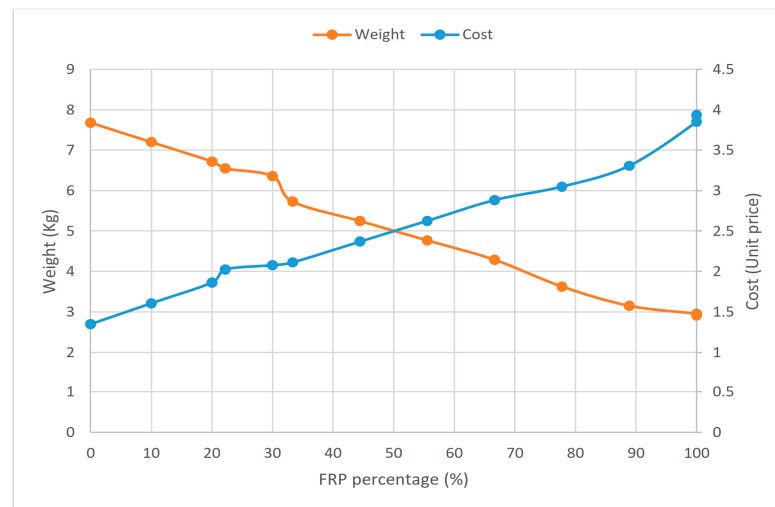


Figure 9. Effect of FRP percentage on weight and cost of the sandwich structure.

6.2. Results of the Finite Element Modeling

To validate the optimization results of the elaborated optimization method, three points on the Pareto front were selected as input parameters for Finite Element simulations. These 3 points were chosen to represent (1) the minimal weight design (single weight optimization), (2) the minimal cost (single cost optimization), and (3) the knee point (multi-objective cost and weight optimization) that provides a compromise between cost and weight.

The FE simulations focused on two outcomes, namely maximal structural deflection and maximal face sheet stress. Contour profiles depicted in Figures 10–15 indicated that the structure experiences the highest deflection and compression stress on the upper face sheet at the mid region of the structure.

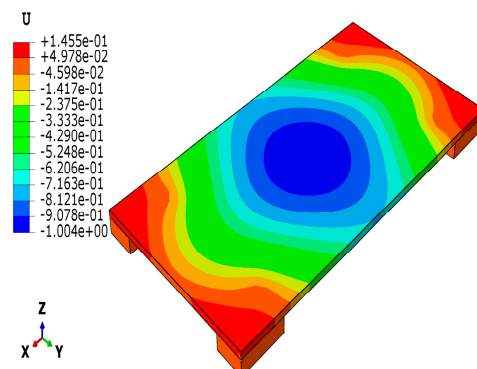


Figure 10. FE contour deflection in case of minimal weight.

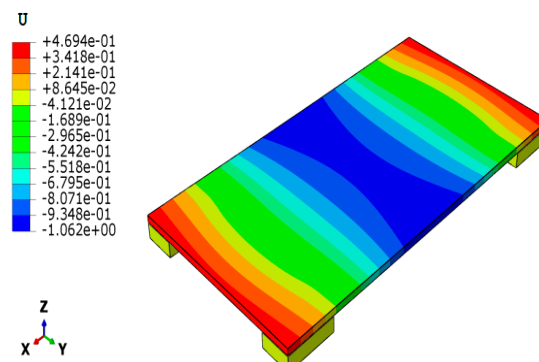


Figure 11. FE contour deflection in case of minimal cost.

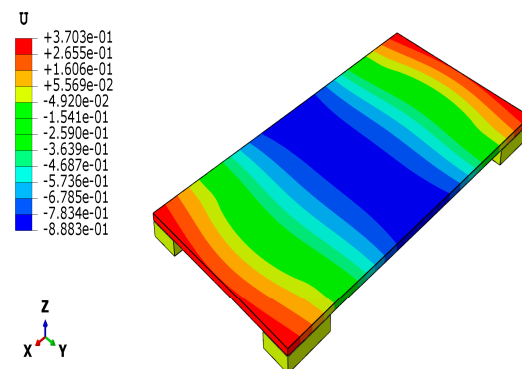


Figure 12. FE contour deflection (K=knee point) in case of multi-objective optimization.

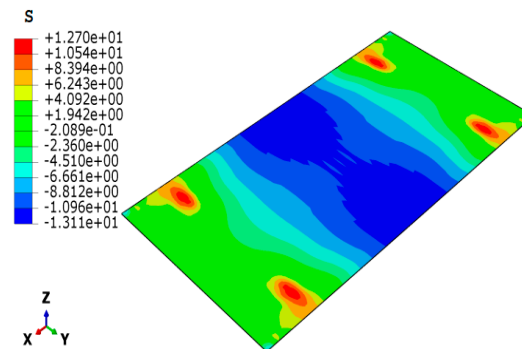


Figure 13. FE contour stress in case of minimal weight.

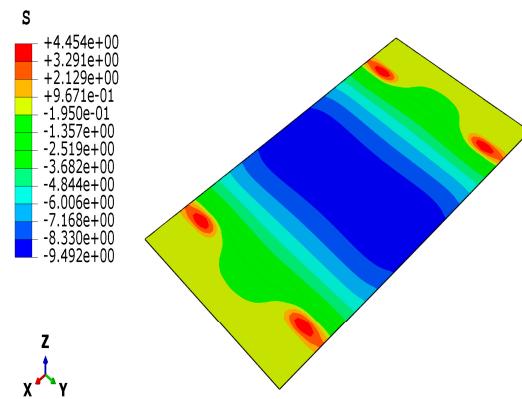


Figure 14. FE contour stress in case of minimal cost.

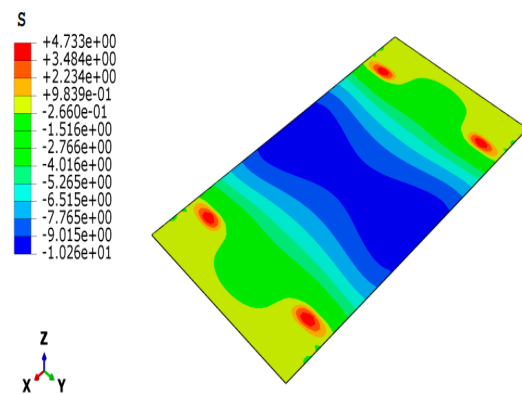


Figure 15. FE contour stress (knee point) in case of multi-objective optimization.

6.3. Comparison of the Optimization Results and the FE Simulation Outcomes

A comparison of the optimization results and the FE simulation outcomes was conducted and presented in Table 7. The outcomes exhibited a good agreement between the two sets of results, indicating that the elaborated optimization results were reliable and accurate with only minor discrepancies.

Table 7. Comparisons of optimization and FE solutions.

Design Points	Maximal Deflection (mm)			Maximal Stress in the Face Sheet (MPa)			Remarks
	Optimization Result	FEM Result	Difference (%)	Optimization Result	FEM Result	Difference (%)	
Minimal weight	0.9957	1.004	0.83	13.655	13.11	3.99	single weight optimization
Minimal cost	1	1.062	6.20	8.695	9.49	9.14	single cost optimization
Knee point	0.9999	0.883	11.69	11.3333	10.26	9.47	multi-objective weight and cost optimization

Consequently, based on the agreement between the numerical optimization and FE simulation results, it is reasonable to conclude that the outcomes of the elaborated optimization method are accurate and reliable.

7. Conclusions

Optimization of weight and cost is considered a crucial factor in designing high-speed trains. Advanced composite sandwich structures have been studied as a viable solution to achieve a lighter train floor in order to reduce the energy consumption of the vehicle.

Although studies on optimizing weight and cost for high-speed train floors are still limited, it is evident that many researchers have implemented weight-saving techniques in the railcar industry through the use of composite structures. For instance, a weight reduction of 40% was achieved in [20], while a reduction of 29% was achieved in [16]. These results highlight the strong motivation to discover innovative design techniques in this field.

The purpose of our study was to develop a multi-objective weight and cost optimization method for high-speed train floors. The sandwich floor structure to be optimized consists of laminated face sheets and a hexagonal honeycomb core. During the optimization different variations of Fiber Metal Laminates (FMLs) as face sheet constructions with aluminum honeycomb cores were examined. The aim of the structural optimization was to construct the optimal sandwich structure in order to provide the minimal weight and minimal cost of the structure. In the optimization, the elaborated weight and cost objective functions, as well as five design constraints, were applied. The Neighborhood Cultivation Genetic (NCGA) algorithm was used to solve the optimization task.

Using the NCGA optimization algorithm resulted in obtaining approximately 16,600 feasible designs that satisfied the design constraints; of these, 13 were characterized as Pareto optimal solutions. A comprehensive analysis of the Pareto optimal solutions was conducted to investigate the correlation between weight and cost objectives. The main findings of this study can be summarized as follows:

- The analysis showed that, at the expense of cost, using CFRP as a face sheet provided a maximum weight reduction of about 62% in this study, compared to the aluminum face sheet as a basic structure.
- Furthermore, a knee point was identified that strikes a balance between weight and cost, resulting in a weight reduction of approximately 32% by using FML materials. This provides valuable insights for designers who must consider both weight savings and cost-effectiveness when designing high-speed train floors.

- The present study conducted an optimization process and subsequently validated its outcomes through Finite Element (FE) simulations. The results of the analysis indicated that there was an acceptable level of agreement between the optimization process and the FE simulations with a maximum difference value of about 11%. This provides a reasonable level of confidence in the obtained results.

To conclude, the proposed multi-objective optimization method utilizing the NCGA algorithm with diverse constituent materials and structural components presents a novel contribution in the context of weight reduction and cost-effectiveness, which has not been previously explored.

The results of this research suggested that sandwich configurations using composite materials are a promising approach to realize lightweight and cost-effective train floors. By using low-density core materials and stiff outer skins, it is possible to achieve an optimal balance between weight reduction, structural performance, and cost efficiency.

The main added value of this study is the elaboration of a multi-objective optimization method that utilizes a wide range of constituent materials and structural components in order to construct the optimal sandwich structure. During the structural optimization, the elaborated weight and cost objective functions, as well as five design constraints, were taken into consideration, applying the NCGA optimization method in order to determine the most cost-effective and lightweight sandwich structure for a given practical application.

In future research based on the elaborated optimization method, more complex structures can be investigated and optimized for other engineering applications. Furthermore, additional design constraints and other materials can be used during the optimization.

Author Contributions: Conceptualization, M.M.S.; literature review, M.M.S.; methodology, M.M.S. and G.K.; formal analysis, M.M.S. and G.K.; visualization, M.M.S.; writing—original draft preparation, M.M.S.; writing—review and editing, M.M.S. and G.K.; supervision, G.K.; invited author, G.K. All authors have read and agreed to the published version of the manuscript.

Funding: This research received no external funding.

Institutional Review Board Statement: Not applicable.

Informed Consent Statement: Not applicable.

Data Availability Statement: Not applicable.

Acknowledgments: The research was supported by the Hungarian National Research, Development and Innovation Office (NKFIH) under the project number K 134358.

Conflicts of Interest: The authors declare no conflict of interest.

References

1. Qi, D.; Sun, Q.; Zhang, S.; Wang, Y.; Zhou, X. Buckling analysis of a composite honeycomb reinforced sandwich embedded with viscoelastic damping material. *Appl. Sci.* **2022**, *12*, 10366. [\[CrossRef\]](#)
2. Jin, X.S. Key problems faced in high-speed train operation. *J. Zhejiang Univ. Sci. A* **2014**, *15*, 936–945. [\[CrossRef\]](#)
3. Zhang, J.; Xiao, X.; Sheng, X.; Zhang, C.; Wang, R.; Jin, X. SEA and contribution analysis for interior noise of a high speed train. *Appl. Acoust.* **2016**, *112*, 158–170. [\[CrossRef\]](#)
4. Mistry, P.J.; Johnson, M.S.; McRobie, C.A.; Jones, I.A. Design of a lightweight multifunctional composite railway axle utilising coaxial skins. *J. Compos. Sci.* **2021**, *5*, 77. [\[CrossRef\]](#)
5. Virág, Z.; Jármai, K. Optimum design of stiffened plates for static or dynamic loadings using different ribs. *Struct. Eng. Mech.* **2020**, *74*, 255–266.
6. Khosravani, M.R.; Weinberg, K. Characterization of sandwich composite T-joints under different ageing conditions. *Compos. Struct.* **2018**, *197*, 80–88. [\[CrossRef\]](#)
7. Feng, Y.; Qiu, H.; Gao, Y.; Zheng, H.; Tan, J. Creative design for sandwich structures: A review. *Int. J. Adv. Robot. Syst.* **2020**, *17*, 1729881420921327. [\[CrossRef\]](#)
8. SBrückmann, M.; Friedrich, H.E.; Kriescher, M.; Kopp, G.; Gätzi, R. Lightweight sandwich structures in innovative vehicle design under crash load cases. *Mater. Sci. Forum* **2017**, *879*, 2419–2427. [\[CrossRef\]](#)
9. Hagnell, M.K.; Kumaraswamy, S.; Nyman, T.; Åkermo, M. From aviation to automotive—A study on material selection and its implication on cost and weight efficient structural composite and sandwich designs. *Heliyon* **2020**, *6*, e03716. [\[CrossRef\]](#) [\[PubMed\]](#)

10. Sayyad, A.S.; Ghugal, Y.M. Bending, buckling and free vibration of laminated composite and sandwich beams: A critical review of literature. *Compos. Struct.* **2017**, *171*, 486–504. [\[CrossRef\]](#)
11. Liu, Q.; Fu, J.; Wang, J.; Ma, J.; Chen, H.; Li, Q. Hui, Axial and lateral crushing responses of aluminum honeycombs filled with EPP foam. *Compos. Part B Eng.* **2017**, *130*, 236–247. [\[CrossRef\]](#)
12. Kwon, D.J.; Kim, J.H.; Devries, K.L.; Park, J.M. Optimized epoxy foam interface of CFRP/Epoxy Foam/CFRP sandwich composites for improving compressive and impact properties. *J. Mater. Res. Technol.* **2021**, *11*, 62–71. [\[CrossRef\]](#)
13. Sahib, M.M.; Kovács, G.; Szávai, S. Optimum Design for the Bottom Panel of a Heavy-Duty Truck by Using a Composite Sandwich Structure. In *Vehicle and Automotive Engineering 4: Select Proceedings of the 4th VAE2022, Miskolc, Hungary*; Springer: Cham, Switzerland, 2022; pp. 734–746.
14. Seyyedrahmani, F.; Shahabad, P.K.; Serhat, G.; Bediz, B.; Basdogan, I. Multi-objective optimization of composite sandwich panels using lamination parameters and spectral Chebyshev method. *Compos. Struct.* **2022**, *289*, 115417. [\[CrossRef\]](#)
15. Manalo, A.; Aravinthan, T. Behavior of Full-Scale Railway Turnout Sleepers from Glue-Laminated Fiber Composite Sandwich Structures. *J. Compos. Constr.* **2012**, *16*, 724–736. [\[CrossRef\]](#)
16. Cho, J.G.; Koo, J.S.; Jung, H.S. A lightweight design approach for an EMU carbody using a material selection method and size optimization. *J. Mech. Sci. Technol.* **2016**, *30*, 673–681. [\[CrossRef\]](#)
17. Zinno, A.; Fusco, E.; Prota, A.; Manfredi, G. Multiscale approach for the design of composite sandwich structures for train application. *Compos. Struct.* **2010**, *92*, 2208–2219. [\[CrossRef\]](#)
18. Heller, P.; Korinek, J.; Triska, L. Hybrid body of underground railway car: Path towards reduced weight of rail vehicles. *Mod. Mach. Sci. J.* **2015**, *2015*, 631–634. [\[CrossRef\]](#)
19. Yao, D.; Zhang, J.; Wang, R.Q.; Xiao, X.B.; Guo, J.Q. Lightweight design and sound insulation characteristic optimisation of railway floating floor structures. *Appl. Acoust.* **2019**, *156*, 66–77. [\[CrossRef\]](#)
20. Wennberg, D.; Stichel, S. Multi-functional design of a composite high-speed train body structure. *Struct. Multidiscip. Optim.* **2014**, *50*, 475–488. [\[CrossRef\]](#)
21. Mozafari, H.; Khatami, S.; Molatefi, H. Out of plane crushing and local stiffness determination of proposed foam filled sandwich panel for Korean Tilting Train eXpress—Numerical study. *Mater. Des.* **2015**, *66*, 400–411. [\[CrossRef\]](#)
22. Zhong, L.; Guo, L.; Li, Y.; Wang, C. Local anti-ablation modification of uneven-density C/C composites with the ZrC-SiC composite ceramics. *Mater. Charact.* **2023**, *198*, 112722. [\[CrossRef\]](#)
23. De Cicco, D.D.; Taheri, F. Delamination buckling and crack propagation simulations in fiber-metal laminates using xFEM and cohesive elements. *Appl. Sci.* **2018**, *8*, 2440. [\[CrossRef\]](#)
24. Gao, S.; Hou, W.; Xing, J.; Sang, L. Numerical and experimental investigation of flexural properties and damage behavior of CFRTP/Al laminates with different stacking sequence. *Appl. Sci.* **2023**, *13*, 1667. [\[CrossRef\]](#)
25. Vieira, L.M.G.; Dobah, Y.; Santos, J.C.D.; Panzera, T.H.; Rubio, J.C.C.; Scarpa, F. Impact properties of novel natural fibre metal laminated composite materials. *Appl. Sci.* **2022**, *12*, 1869. [\[CrossRef\]](#)
26. Chang, H.; Zhang, L.; Dou, W.; Zhang, H. Improved strategies for the load-bearing capacity of aluminum-PVC foam sandwich floors of a high-speed train. *J. Mech. Sci. Technol.* **2021**, *35*, 651–659. [\[CrossRef\]](#)
27. Nestler, D.; Trautmann, M.; Zopp, C.; Tröltzsch, J.; Osiecki, T.; Nendel, S.; Wagner, G.; Kroll, L. Continuous film stacking and thermoforming process for hybrid CFRP/aluminum laminates. *Procedia CIRP* **2017**, *66*, 107–112. [\[CrossRef\]](#)
28. Baumert, E.K.; Johnson, W.S.; Cano, R.J.; Jensen, B.J.; Weiser, E.S. Mechanical evaluation of new fiber metal laminates made by the VARTM process. In *Proceedings of the 17th International Conference on Composite Materials (ICCM), Edinburgh, UK, 27–31 July 2009*.
29. HexCel Composites, Honeycomb Sandwich Design Technology. 2000. Available online: https://www.hexcel.com/user_area/content_media/raw/Honeycomb_Sandwich_Design_Technology.pdf (accessed on 20 February 2023).
30. Watanabe, S.; Hiroyasu, T.; Miki, M. NCGA: Neighborhood cultivation genetic algorithm for multi-objective optimization problems. *Proc. Genet. Evol. Comput. Conf.* **2002**, *43*, 465–468.
31. Chen, Y.; Fu, K.; Hou, S.; Han, X.; Ye, L. Multi-objective optimization for designing a composite sandwich structure under normal and 45° impact loadings. *Compos. Part B Eng.* **2018**, *142*, 159–170. [\[CrossRef\]](#)
32. Duan, S.; Tao, Y.; Han, X.; Yang, X.; Hou, S.; Hu, Z. Investigation on structure optimization of crashworthiness of fiber reinforced polymers materials. *Compos. Part B Eng.* **2014**, *60*, 471–478. [\[CrossRef\]](#)
33. Chen, Y.; Liu, G.; Zhang, Z.; Hou, S. Integrated design technique for materials and structures of vehicle body under crash safety considerations. *Struct. Multidiscip. Optim.* **2017**, *56*, 455–472. [\[CrossRef\]](#)
34. Zenkert, D. *An Introduction to Sandwich Construction*; Engineering Materials Advisory Services (EMAS): London, UK; Stockholm, Sweden, 1995.
35. Kollar, L.P.; Springer, G.S. *Mechanics of Composite Structures*, 1st ed.; Cambridge University Press: Cambridge, UK, 2003.
36. Kaw, A.K. *Mechanics of Composite Materials*; Taylor & Francis: New York, NY, USA, 2005.
37. Hudson, C.W.; Carruthers, J.J.; Robinson, A.M. Multiple objective optimisation of composite sandwich structures for rail vehicle floor panels. *Compos. Struct.* **2010**, *92*, 2077–2082. [\[CrossRef\]](#)

38. Barbero, E.J. *Finite Element Analysis of Composite Materials Using AbaqusTM*, 2nd ed.; Taylor & Francis: New York, NY, USA, 2013.
39. Yuan, J.; Zhang, L.; Huo, Z. An equivalent modeling method for honeycomb sandwich structure based on orthogonal anisotropic solid element. *Int. J. Aeronaut. Space Sci.* **2020**, *21*, 957–969. [[CrossRef](#)]

Disclaimer/Publisher's Note: The statements, opinions and data contained in all publications are solely those of the individual author(s) and contributor(s) and not of MDPI and/or the editor(s). MDPI and/or the editor(s) disclaim responsibility for any injury to people or property resulting from any ideas, methods, instructions or products referred to in the content.